THE JOURNAL OF PHYSICAL CHEMISTRY C

Article

pubs.acs.org/JPCC

Can Mixed-Metal Surfaces Provide an Additional Enhancement to SERS?

Roberto Olivares-Amaya,[†] Dmitrij Rappoport,[†] Philip A. Munoz,[‡] Paul Peng,[‡] Eric Mazur,[‡] and Alán Aspuru-Guzik*,[†]

[†]Department of Chemistry and Chemical Biology, and [‡]School of Engineering and Applied Sciences, Harvard University, Cambridge, Massachusetts 02138, United States

Supporting Information

ABSTRACT: We explore the chemical contribution to surface-enhanced Raman scattering (SERS) in mixed-metal substrates, both experimentally and by computer simulation. These substrates are composed of a chemically active, transition-metal overlayer deposited on an effective SERS substrate. We report improved analytical enhancement factors obtained by using a small surface coverage of palladium or platinum over nanostructured silver substrates. Theoretical predictions of the chemical contribution to the surface enhancement using density functional theory support the experimental results. In addition, these approaches show that the increased enhancement is due not only to an increase in surface coverage of the analyte but also to a higher Raman scattering cross section per molecule. The additional chemical enhancement in mixed-metal SERS substrates correlates with the binding energy of the analyte on the surface and includes both static and dynamical effects. SERS using mixed-metal substrates has the potential to improve sensing for a large group of analyte molecules and to aid the development of chemically specific SERS-based sensors.

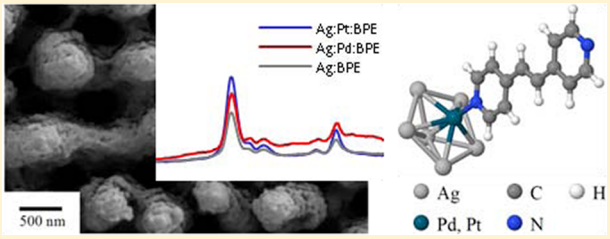

INTRODUCTION

Surface-enhanced Raman scattering (SERS) is observed in molecules deposited on rough or nanostructured metal surfaces.[1−5] Over the past decade, SERS has developed into a powerful analytical technique.[6−10] The enormous enhancement of the ordinarily weak Raman scattering cross sections in SERS is attributed to two main effects: electromagnetic and chemical enhancement. Electromagnetic enhancement is due to the presence of strong electromagnetic fields at the surface of nanoscale metal particles and is responsible for enhancements of Raman scattering cross sections of 10 or more orders of magnitude.[6,7] Chemical enhancement is related to the formation of chemical bonds between the adsorbed molecule and surface metal atoms.[11−16] While being much smaller in absolute magnitude than the electromagnetic effect, chemical enhancement has important implications for SERS as an analytical tool and can provide up to 2−3 orders of magnitude of enhancement in addition to the electromagnetic contribution. Furthermore, it affects Raman-active vibrations selectively and thus alters the shapes of Raman spectra in addition to providing enhancement.[17] Last, the chemical effect is chemically specific and has potential for improved performance of SERS in analytical applications. The exact origin of the chemical contribution to surface enhancement remains an active area of research in both theory and experiment.[4,5,11,12,14−16,18−21] Chemical enhancement can be modeled as a combination of a static contribution connected to the redistribution of electron density between the metal and the molecule and a dynamical contribution arising from resonance enhancement due to surface excited states of mixed metal-molecular character.[16]

Gold and silver are the most commonly used substrate materials for SERS applications. Ag has been found to give highest enhancements of Raman cross sections for an excitation in the visible range, while Au is often used because of simpler processing and resistance to oxidation. Recently, Wang et al. have created nanostructured silicon and germanium-based SERS substrates.[22,23] For these structures, the enhancement is in the order of 10^2−10^4. Its enhancement mechanism relies on a photon-induced charge transfer process instead of the typical plasmon-based approach. Although this effect is by no means as intense as with Ag and Au, it provides evidence that these materials can provide a SERS signal despite the lack of plasmonic properties.

Several other metals have been explored with regard to surface enhancement.[24] Differences in the localized surface-plasmon resonances (LSPR) in scattering and absorption spectra of these metals relative to the frequencies of the incident and scattered radiation result in vastly different electromagnetic enhancements.[4] On the other hand, the richness of chemical reactivity of transition metals opens the prospect of chemically selective binding and detection.

The idea of using mixed-metal substrates, which combine the SERS activity of a majority metal (typically a coinage metal)

Received: March 18, 2012
Revised: May 31, 2012
Published: June 8, 2012

with the chemical properties of a dopant metal (deposited as an overlayer), was proposed early on.[25−28] In subsequent extensive work of Weaver, Tian, Dai, et al., fabrication techniques for producing transition- and mixed-metal substrates were considerably improved, and their surface enhancements were explored in great detail.[29−38] Their work was motivated by the concept of SERS borrowing, originally put forward by Van Duyne and Haushalter.[39] SERS borrowing refers to the fact that dopant metals are poor SERS substrates by themselves. However, when deposited as an overlayer atop effective SERS substrates to probe catalytic reactions, or as a protective overlayer, they acquire some surface enhancement "borrowed" from the coinage metal. If only the electromagnetic enhancement is taken into account, one expects the enhancement factors for these mixed-metal substrates to be lower than for pure coinage metals. The attenuation of the surface enhancement has been described in terms of the distance dependence of the electromagnetic fields and has been broadly explored.[29,40−43] The above picture neglects the effect of the strong coordinative bonds formed between the dopant metal and specific analytes, for example, pyridine. Therefore, the objective of this work is to explore, both experimentally and using simulation, the chemical contribution to surface enhancement in mixed-metal SERS substrates.

We expect that stronger chemical bonding in suitably chosen mixed-metal substrates, coupled with existing advanced nanofabrication techniques, can help to balance or in ideal cases even overcome the attenuation of electromagnetic enhancement. In this case, we propose and coin the term of an additional SERS lending effect, where the transition-metal overlayer could contribute to the overall surface enhancement due to the strong chemical bonding. SERS lending would open an avenue for new analytical applications of SERS. Well-known and recent results from surface chemistry[44−48] may serve as an inspiration for designing new mixed-metal SERS substrates. In particular, transition metals of the nickel group are known to form strong coordinative bonds with nitrogen-containing molecules and are promising candidates for their detection with SERS. In contrast, gold and silver substrates tend to bind more strongly to thiols. As mentioned above, mixed-metal substrates using nickel, palladium, and platinum were extensively studied by Weaver, Tian, et al. in the context of SERS borrowing.[29,32,35−37] Furthermore, molybdenum-covered SERS substrates could possibly be used for improved chemical bonding to oxygen-containing molecules.

The effect of stronger chemical bonding between the analyte and the metal surface on the Raman signal is 2-fold. A stronger binding affinity results in a higher concentration of the analyte on the surface, which yields higher analytical enhancements. In addition, stronger coupling between the electronic structure of metal surface and vibrations of the molecule leads to an enhancement of the Raman cross section per molecule. These effects have to be balanced with the damping of the plasmonic resonance due to the presence of the dopant metal as well as changes in surface morphology in mixed-metal SERS substrates. A complete investigation of all of these effects presents a number of challenges. In this work, we explore the chemical enhancement in mixed-metal clusters using theoretical models to describe the coupling between the analyte and the metal surface. As was shown in previous studies, chemical enhancement in SERS depends mainly on the immediate chemical environment of the binding site and can be successfully modeled using cluster models.[16,49]

In the following, we present Raman scattering calculations of *trans*-1,2-bis(4-pyridyl) ethylene (BPE) on silver-based mixed-metal clusters to theoretically characterize the chemical contribution to surface enhancement. We report experimental measurements of BPE on Ag substrates with nanometer-thick overlayers of Pd or Pt. Further computational results predict that similar effects are possible with Au as majority metal and Pd or Pt as dopant metals. Finally, we study the electronic effects of mixed-metal SERS by analyzing the Raman excitation profile of pyridine (Py) bound to silver to explore the dynamical contribution to the chemical enhancement in mixed-metal SERS substrates.

EXPERIMENTAL METHODS

SERS Substrate Fabrication. Experimental Raman spectra are collected from BPE adsorbed onto a femtosecond laser nanostructured SERS substrate, using the setup previously reported in ref 50 . This type of substrate has been previously shown to provide SERS enhancement factors of 10^9, relative to pure analyte.[50,51] All substrates were fabricated using a femtosecond laser structuring process on a n-type silicon (100) wafer (ρ = 0.005−0.020 Ω cm). A pulse train from a regeneratively amplified titanium:sapphire laser was used to generate 800 nm center wavelength, 100 fs pulses at a repetition rate of 1 kHz. This pulse train was frequency-doubled to a center wavelength of 400 nm using a thin $BiBO_3$ crystal. The second harmonic pulse width exiting the crystal was less than 200 fs. These laser pulses were loosely focused with a plano-convex lens to achieve an average fluence of 10 kJ m^{-2} at the surface of a silicon wafer fastened to the inside of a 10 mm deep cuvette filled with deionized water. The cuvette was mounted on a computer-controlled two-axis translation stage and rastered at an appropriate speed such that each point on the silicon wafer was subjected to approximately 500 pulses.

To render the surfaces SERS-active, silver was thermally evaporated onto the structured silicon. Using a quartz crystal microbalance to measure the thickness of a planar continuous film, substrates were fabricated with 80 nm of deposited silver. All films were thermally evaporated at a rate of 0.15 nm s^{-1}, with no heating or cooling applied to the substrate during deposition. A subsequent layer of 1−4 nm of platinum or palladium is added to probe the mixed-metal effects. The metal-coated substrates were submerged in 10 μM solutions of BPE made with ethanol for 1 h and then gently rinsed in ethanol for 1 min, followed by drying under a stream of nitrogen.

Raman Spectroscopy. Using a 5 mW, s-polarized HeNe laser, spectra were recorded through a 10× microscope objective (0.25 NA) and projected onto a thermoelectrically cooled charged-couple device array using 1200 mm^{-1} diffraction grating. Individual spectra were recorded from both single spots (1.6 μm diameter) on the substrate, and from a 500 μm thick cell of neat BPE for normalization.

Electron Microscopy. Secondary electron microscope images of the substrates were collected using a field-emission gun scanning electron microscope, utilizing an accelerating voltage of 5 kV. No additional sample preparation was performed prior to imaging the substrates.

THEORETICAL METHODS

Computational Details. Density-functional calculations were performed using the PBE0 functional.[52] Triple-ζ valence basis sets with one set of polarization functions (def2-TZVP)

dx.doi.org/10.1021/jp302597v | J. Phys. Chem. C 2012, 116, 15568−15575

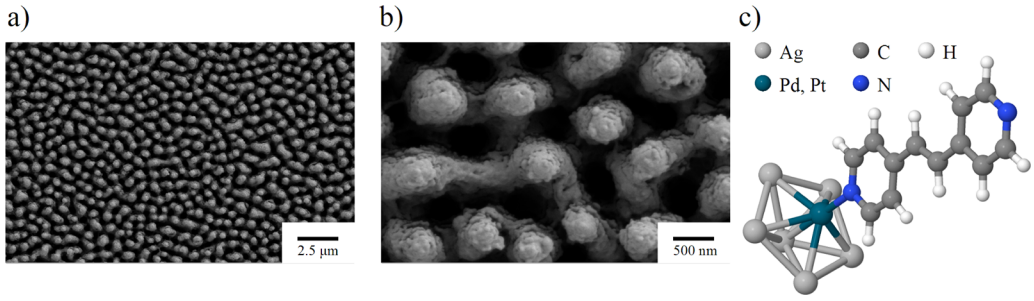

Figure 1. (a,b) SEM pictures of a femtosecond laser nanostructured SERS substrate and 2 nm Pt overlayer thermally evaporated on top of the substrate. (c) Structure of a Ag_6M·BPE complex.

and split-valence basis sets with polarization (def2-SVP) were used for the main group and transition metal elements, respectively.[53] Relativistic effective core potentials (ECP) comprising 28 core electrons for Ag and Pd and 60 core electrons were employed for Au and Pt, respectively.[54] The PBE0 functional was chosen because it has proven to be accurate for polarizabilities[55,56] and Raman intensities,[57,58] although it is known to overestimate vibrational frequencies[59] and electronic excitation energies.[60] The Turbomole package[61] was used to perform all calculations.

Raman Scattering Calculations. Raman intensities were computed using the static polarizability limit, except for the Raman intensities calculated for the Raman excitation profiles.[57] No scaling of vibrational frequencies was applied. The Raman spectra were simulated by Lorentzian broadening of the line spectra using an empirical line width of 5 cm^{-1}. A scattering angle of 90° and perpendicular polarization of both incident and scattered radiation were employed.

Geometry Optimization and Energy Calculations. The molecular systems were relaxed using the PBE0 functional. Multiple spin geometries were studied, and singlets (doublets in the open-shell case) were most stable. The molecule-cluster systems presented an imaginary mode, even after repeated attempts to relax the molecule. This mode was prevalent at the 3−15 cm^{-1} region. None of the bare clusters or molecules presented imaginary frequencies. Cartesian coordinates of the minimized structures are provided in the Supporting Information. We performed binding energy calculations. We neglected the basis set superposition error as it has been previously estimated to be 0.03 eV for the binding of pyridine with a Ag_{20} cluster.[49]

RESULTS

I. Enhancement Effects of BPE Using Mixed-Metal Substrates. We prepared silver-based SERS substrates including a thin overlayer of Pd or Pt. Details regarding the nanofabrication of these surfaces can be found in the Experimental Methods. Silicon surfaces were roughened by a femtosecond laser nanostructuring process.[50] An 80 nm thick layer of silver was deposited on the roughened surfaces by thermal evaporation; subsequently, an overlayer of Pd or Pt of 1−4 nm thickness was created by the same technique. In Figure 1a,b, we show scanning electron microscope (SEM) images of the silver substrate with 2 nm Pt coverage. We notice a similar quasi-uniform distribution of raised features as shown in the work by Diebold et al.,[50] even in the presence of an additional transition metal.

Thermal evaporation is a highly directional process that preferentially coats the top surface of the sample and may leave shadows exposed to Ag. There have been previous efforts to ensure a pinhole free surface in an electrochemical setting by Weaver et al.[30] We currently do not explore these or other possible chemical methods.[33] The current setup to identify elemental composition of surface coverage employs the SEM setup coupled with energy-dispersive X-ray spectrometry (EDS). The latter has a micrometer-sized resolution, so other ways of determining surface coverage, such as chemical probes, are needed.[29]

To elucidate the role of the chemical contribution to surface enhancement in bimetal substrates, we calculated the Raman cross sections of BPE bound to small-cluster models of SERS substrates. We use seven-atom (Ag_6M·BPE) and larger 18-atom cluster ($Ag_{14}M_4$·BPE) models; see Figure 1c. Chemical enhancement effects appear to be well localized around the site of the chemical bond between metal atoms and the analyte molecule. In previous work, these have been shown to provide realistic models for chemical enhancement.[16,17]

The experimental Raman spectrum of BPE at 633 nm excitation wavelength on a silver substrate and the computed Raman spectra for the Ag_7·BPE and Ag_{18}·BPE complexes are compared in Figure 2. The vibrational frequencies and relative

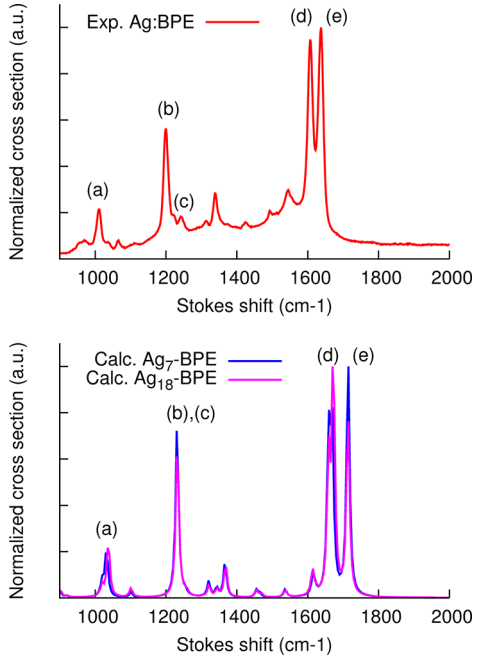

Figure 2. (Top) Experimental Raman spectrum of BPE and 80 nm Ag substrate using 633 nm wavelength. (Bottom) Calculated Raman spectra of Ag_7·BPE and Ag_{18}·BPE complexes.

dx.doi.org/10.1021/jp302597v | J. Phys. Chem. C 2012, 116, 15568−15575

Raman cross sections are in good agreement between the experimental and the computed spectra. In Table 1, we present the five most prominent normal modes of the bare BPE molecule as shown in the Supporting Information and reported elsewhere.[62,63] As BPE interacts with the metal, there is a shift of its normal modes. Also, the peak present at 1232 cm^{-1}, related to scissor C−H vibration in the ring, has a large decrease of its relative intensity. The four most prominent vibrational modes in the surface-enhanced setup are clearly identified as the ring-breathing mode of the pyridine rings at 1010 cm^{-1}, the in-plane bending of the pyridine rings at 1200 cm^{-1}, the ring stretching mode at 1610 cm^{-1}, and the ethylene stretching mode at 1640 cm^{-1}.[62,64] The differences between the two cluster models are comparatively small, with the largest deviations found in the relative Raman cross sections for the 1610 and 1640 cm^{-1} modes. In the following, we will therefore focus only on presenting the results for small (i.e., 7 atom) clusters. The computed vibrational frequencies are overestimated by about 4% by the PBE0 functional used in this work, in accord with previous benchmark studies.[59] For consistency, we do not rescale the calculated frequencies, and the mode assignment in Table 1 should serve as a guide to relate experimental and calculated frequencies.

Table 1. Mode Assignment of the Five Most Prominent Normal Modes of Bare BPE

	mode (cm^{-1})		
	experimental	calculated	assignment
(a)	993.7	1019.8	ring-breathing
(b)	1196.5	1231.0	in-plane bending
(c)	1232.7	1253.1	C−H scissor
(d)	1595.0	1657.6	ring-stretching
(e)	1634.3	1714.5	ethylene-stretching

In Figure 3, we show the experimental Raman spectra of BPE absorbed on the silver SERS substrate and mixed-metal SERS substrates using 1 nm coverage of Pd or Pt at 633 nm excitation wavelength. We observed a stronger Raman signal for mixed-metal SERS substrates as compared to the silver SERS substrate. Also, Pt coverage of 1 nm thickness is more effective in enhancing the Raman signal than Pd coverage of the same thickness. The relative Raman signals from different modes and the shapes of measured Raman spectra remain virtually unchanged. Measurements of Raman cross sections of BPE on SERS substrates are complicated by the fact that its surface coverage is not exactly known and might vary depending on the composition of the SERS substrate. Therefore, we consider analytical enhancement factors (AEF) as defined by LeRu, Etchegoin, and co-workers and used extensively in SERS research:[65−67]

$$\mathrm{AEF} = \frac{I_{\mathrm{SERS}}/c_{\mathrm{SERS}}}{I_{\mathrm{ref}}/c_{\mathrm{ref}}} \quad (1)$$

where I is the Raman intensity and c represents the concentration of the analyte. The significance of the observed analytical enhancement factors is discussed extensively below.

At close to 1 nm thickness, Pd- and Pt-covered substrates show analytical enhancement factors for the 1200 cm^{-1} mode that are 1.4 and 1.8 times higher than that for the silver SERS substrate, respectively. At 2 nm thickness, this ratio drops to 0.75 when using a Pd-covered substrate. The analytical enhancement factor for the 2 nm Pt-covered substrate is 1.9 times higher than for the silver substrate; indicating that there is a sustained enhancement as the coverage thickness increases. We observe no SERS enhancement beyond a layer thickness of 3 nm layer of Pd or Pt (not shown). The dependence of the measured analytical enhancement factors on the thickness of the transition-metal overlayer is summarized in Figure 4.

The computed Raman spectra of the Ag_6M·BPE complexes (M = Ag, Pd, Pt) are shown in Figure 3. Increased Raman cross sections are observed in transition-metal complexes, while relative cross sections are preserved, in line with experimental results. For the in-plane bending mode at 1200 cm^{-1}, we find that replacement of the proximal Ag atom by a Pd atom leads

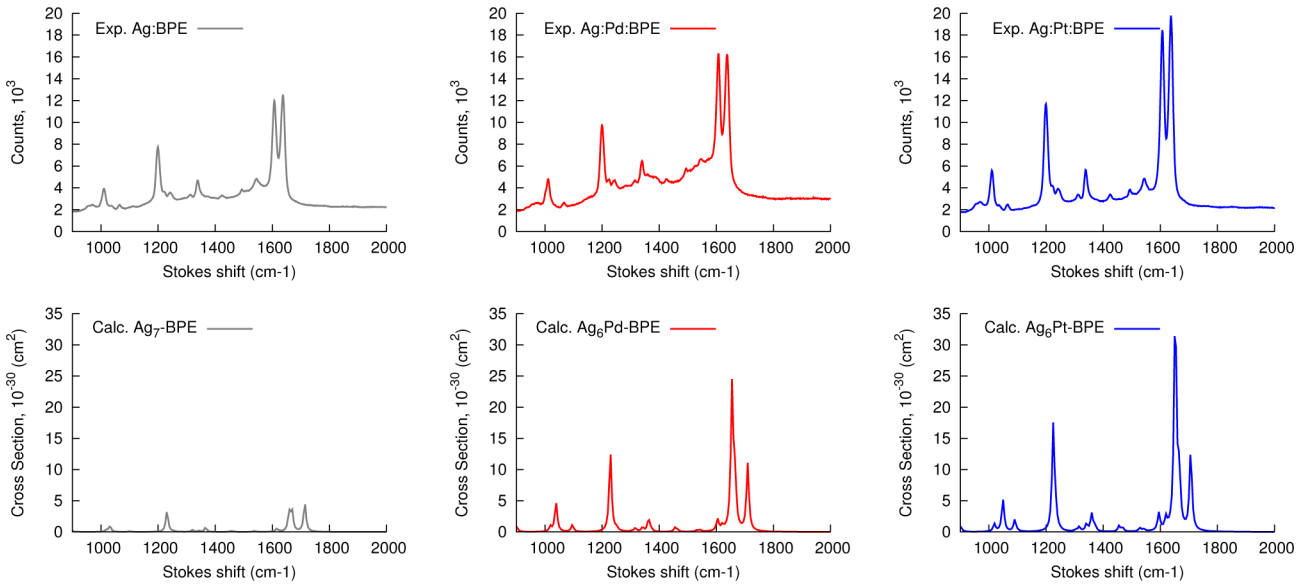

Figure 3. (Top) Experimental and computed SERS spectra of BPE. Experimental Raman scattering cross sections at 633 nm incident wavelength of BPE on 80 nm Ag substrate, 80 nm Ag substrate with 1 nm Pd overlayer, and 80 nm Ag substrate with 1 nm Pt overlayer. (Bottom) Calculated Raman spectra of Ag_7·BPE, Ag_6Pd·BPE, and Ag_6Pt·BPE complexes.

dx.doi.org/10.1021/jp302597v | J. Phys. Chem. C 2012, 116, 15568−15575

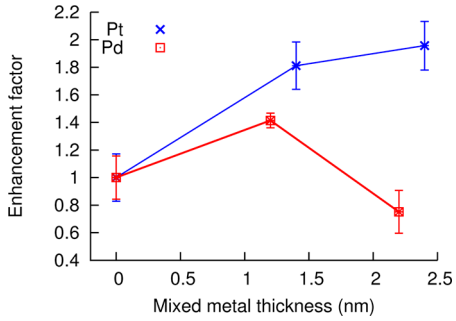

Figure 4. Analytical enhancement factors for the integrated signals of the in-plane bending mode of BPE on mixed-metal SERS substrates as a function of the transition-metal thickness. The analytical enhancement factors are normalized with respect to the silver SERS substrates (0 nm thickness). For Pd coverage, there is only enhancement at 1.2 nm thickness, while the Pt signal is close to 1.9 at both 1.4 and 2.4 nm coverage.

to a 3.8-fold increase in Raman cross section. For the Ag_6Pt·BPE complex, the Raman cross section is highest, 5.1 times higher as compared to the Ag_7·BPE complex. The Raman spectra of the larger complexes of the form, $Ag_{14}M_4$·BPE, show a similar trend and are given in the Supporting Information. The computed results are summarized in Table 2.

Table 2. Enhancement Factors of the In-Plane Bending Mode of Ag_6M·BPE Complexes (Relative to Ag_7·BPE) and $Ag_{14}M_4$·BPE Complexes (Relative to Ag_{18}·BPE)[a]

Ag_6M·BPE	enhancement	ΔE (eV)	Ag_{18}·BPE	enhancement
Ag_7·BPE	1.00	−0.38	Ag_{18}·BPE	1.00
Ag_6Pd·BPE	3.79	−0.92	$Ag_{14}Pd_4$·BPE	2.28
Ag_6Pt·BPE	5.08	−1.41	$Ag_{14}Pt_4$·BPE	4.25

[a]Binding energies ΔE of Ag_6M·BPE complexes according to eq 2.

Nitrogen-containing heterocycles such as BPE are known to form strong coordinative bonds to transition metals of the platinum group. This strong bonding can be expected to have a significant effect on the chemical contribution to surface enhancement. Therefore, it is instructive to study the binding energies of BPE to the mixed-metal clusters as a simple measure of the metal-molecular bonding. The binding energies ΔE are computed as electronic reaction energies (without zero-point correction) of the Ag_xM_y·BPE complex formation:

$$\Delta E = E(Ag_xM_y\cdot BPE) - E(Ag_xM_y) - E(BPE) \quad (2)$$

The binding energies are given in Table 2 and follow the trend Ag < Pd < Pt. This observation is in line with complex stability of transition metals[68−70] and suggests that the mixing between electronic levels in the molecule and the metal cluster is correlated to the increase in Raman scattering cross sections. A simple explanation is that stronger bonding leads to a stronger coupling of vibrational modes in the analyte molecule to the large polarizability of the metal cluster.

Further, we computed Raman spectra of the Au_6M·BPE complexes (M = Au, Pd, Pt) and their binding energies according to eq 2 that are shown in Figure 5 and Table 3. The

Table 3. Enhancement Factors of the In-Plane Bending Mode of Au_6M·BPE Complexes (Relative to Au_7·BPE)[a]

Au_6M·BPE	Enhancement	ΔE (eV)
Au_7·BPE	1.00	−0.64
Au_6Pd·BPE	1.66	−1.05
Au_6Pt·BPE	2.26	−1.67

[a]Binding energies ΔE of Au_6M·BPE complexes according to eq 2.

chemical enhancement and the Raman cross sections increase in the sequence Au < Pd < Pt. The effect of Pd and Pt is, however, smaller than for the Ag_6M·BPE complexes, while the binding energies are similar for both Ag_6M·BPE and Au_6M·BPE series of complexes. It is therefore apparent that other electronic-structure considerations need to be taken into account to fully understand the origin of the mixed-metal effect.

Theory and experiment are complementary in the understanding of the molecule-metal and mixed-metal interface. In this work, we are able to provide analytical enhancement factors, but the surface coverage of BPE on SERS substrates is unknown and its measurement is far from trivial.[71] Theoretical results predict an increase in Raman cross sections per molecule when the analyte binds to a Pd or Pt atom, an effect that can be described by SERS lending. The enhanced Raman cross sections are concomitant with an increase in binding energy between the analyte and the metallic surface. Higher binding energies will however also lead to increased surface coverage of the analyte under equilibrium conditions, potentially yielding higher analytical enhancement factors. Estimating the surface coverage is therefore necessary to interpret the experimental findings.

Previously reported surface coverage experiments of pyridine on roughened electrodes of Ag and Pt yield a coverage of $(4.5–6.5) \times 10^{-10}$ and 5.1×10^{-10} mol cm^{-2}, respectively.[72−74] These measurements were done for a similar bulk concentration of pyridine, although each was determined with a different method. In the case of BPE, estimations of the surface coverage on Ag have relied on a geometric area estimation of 1.16×10^{-9} mol cm^{-2},[75−77] though we note this is likely an overestimate. Measurements of BPE on Pt have reported to give a coverage of 4.75×10^{-10} mol cm^{-2}.[78] Although the

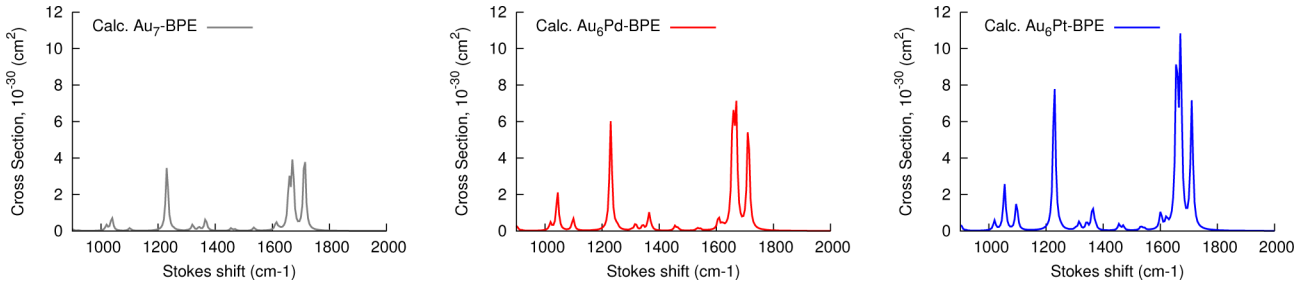

Figure 5. Calculated Raman spectra of Au_7·BPE, Au_6Pd·BPE, and Au_6Pt·BPE complexes.

dx.doi.org/10.1021/jp302597v | J. Phys. Chem. C 2012, 116, 15568−15575

variety of methods shrouds the comparison, the difference in surface coverage between Pt and Ag is not over a factor of 2 greater. Therefore, coverage cannot be the sole factor for the 1.9-fold enhancement we find experimentally. Along with robust theoretical predictions of increased Raman cross sections per molecule, we tentatively conclude that a SERS lending effect is present in mixed-metal substrates considered in this work.

II. Theoretical Study of Pyridine: Raman Excitation Profile. We proceed by investigating the importance of a dynamical contribution to chemical enhancement in mixed-metal clusters using complexes $Ag_6M{\cdot}Py$ as an example. Table 4 shows the relative Raman scattering cross sections for the 1230 cm^{-1} in-plane bending mode of pyridine as well as binding energies computed according to eq 2. This vibration corresponds to the 1200 cm^{-1} mode in BPE (spectra available in the Supporting Information). The binding energies follow the same trends as in the case of BPE and are within 0.04 eV of the values obtained for $Ag_6M{\cdot}BPE$; compare Table 2. The Raman cross section of the 1230 cm^{-1} mode is 6 times higher in $Ag_6Pd{\cdot}Py$ and 9 times higher in $Ag_6Pt{\cdot}Py$ as compared to the $Ag_7{\cdot}Py$ complex. However, the absolute Raman cross-section for this mode is 20 times smaller than in complexes containing BPE (shown in the Supporting Information).

Table 4. Enhancement Factors of the In-Plane Bending Mode of $Ag_6M{\cdot}Py$ Complexes (Relative to $Ag_7{\cdot}Py$)[a]

$Ag_6M{\cdot}Py$	enhancement	ΔE (eV)
$Ag_7{\cdot}Py$	1.00	−0.38
$Ag_6Pd{\cdot}Py$	6.10	−0.90
$Ag_6Pt{\cdot}Py$	9.27	−1.37

[a]Binding energies ΔE of $Ag_6M{\cdot}BPE$ complexes according to eq 2.

Raman excitation profiles (REPs) are a useful tool in elucidating the dynamical contribution surface enhancement and describe the dependence of Raman cross sections on the excitation frequency.[16] In Figure 6, we show REPs for the ring-breathing mode (experimental frequency 990 cm^{-1}) and the in-plane bending mode (1200 cm^{-1}) of $Ag_6Pt{\cdot}Py$ and $Au_6Pt{\cdot}Py$ complexes. The silver−platinum complex has its lowest-energy electronic excitation at 607 nm, while the lowest excitation occurs at 616 nm in the gold−platinum complex. For both vibrational modes, $Ag_6Pt{\cdot}Py$ exhibits a large increase in Raman cross sections close to the electronic excitation at 607 nm, showing almost an order of magnitude increase in Raman cross section for the ring-breathing mode. In contrast, $Au_6Pt{\cdot}Py$ complex fails to show a significant increase for both of these modes at its excitation wavelength of 616 nm.

Isosurface plots of transition electron densities for the lowest-energy excitations in $Ag_6Pt{\cdot}Py$ and $Au_6Pt{\cdot}Py$ are displayed in Figure 6. In the case of $Ag_6Pt{\cdot}Py$ (Figure 7a), the transition density lies exactly at the metal−molecule interface. The $Au_6Pt{\cdot}Py$ complex (Figure 7b) is characterized by a transition density that is spread throughout the metal cluster. These observations provide a simple explanation for the computed REPs of Figure 6. We note that when an excitation transition density is largely localized at the metal−molecule interface, the Raman cross sections for excitation energies close to it are strongly enhanced, as has been reported previously for Ag_n−SPh complexes.[16] In contrast, excitations in the metal cluster have a much smaller effect on Raman cross sections. The differences between Au and Ag as majority metals illustrate that excited-state properties are also important to understand the effects in mixed-metal systems.

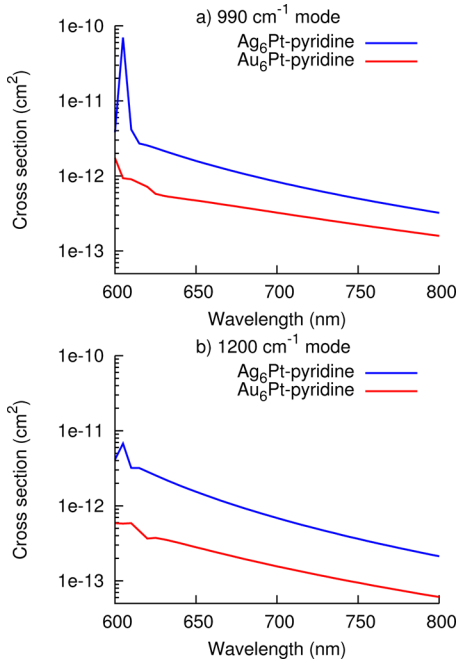

Figure 6. Raman excitation profiles (REP) of ring-breathing mode (990 cm^{-1}, a) and in-plane bending mode (1200 cm^{-1}, b) of pyridine in $Ag_6Pt{\cdot}Py$ and $Au_6Pt{\cdot}Py$ complexes.

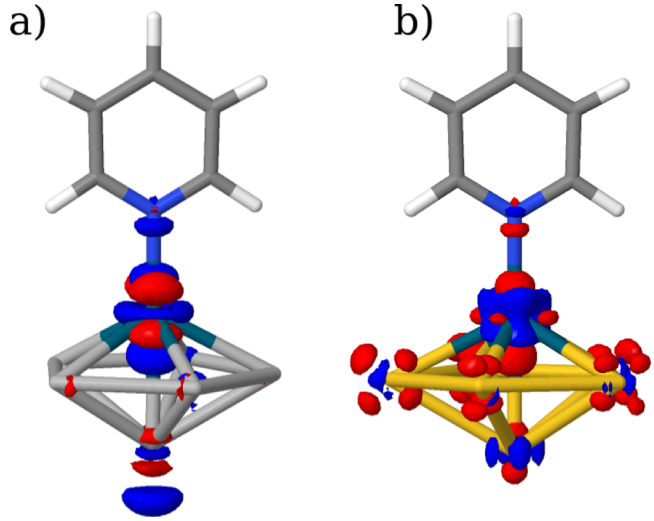

Figure 7. Isosurface plots of computed transition densities of lowest-energy electronic excitations in $Ag_6Pt{\cdot}Py$ (excitation wavelength 607 nm, a) and $Au_6Pt{\cdot}Py$ complex (excitation wavelength 616 nm, b). The red color indicates a transition density of −0.005 au, while the blue corresponds to a transition density of 0.005 au.

CONCLUSIONS

The chemical contribution to surface enhancement in mixed-metal SERS substrates was investigated by experimental and theoretical techniques. We report an increase by up to 1.9-fold in analytical enhancement factors obtained experimentally for BPE on silver-based SERS substrates including an overlayer of Pd or Pt of 1−2 nm thickness. The analytical enhancement factors include the effect of surface coverage of the analyte, the attenuation of the electromagnetic enhancement by the

dx.doi.org/10.1021/jp302597v | J. Phys. Chem. C 2012, 116, 15568−15575

transition-metal overlayer, as well as changes in the chemical enhancement. The observed increase in analytical enhancement factors is unlikely to arise solely from a higher surface coverage on Pd- or Pt-containing SERS substrates. Therefore, we conclude that a SERS lending effect is present in mixed-metal SERS substrates due to an increase in chemical enhancement.

These findings are further corroborated by theoretical results on small-cluster models, which consistently predict up to a 5-fold increase in Raman cross sections for BPE on Pd- or Pt-containing mixed-metal clusters. The differences in enhancement are understandable because the theoretical model does not take into account the distance-dependent decrease of electromagnetic enhancement (i.e., plasmon decay). It is likely the issue of the attenuation of the electromagnetic effect can be alleviated.[41,42,79] Overall, the enhancement is a combination of the attenuation and the chemical enhancement effect. As mentioned above, the chemical enhancement can lead to observable SERS spectra without necessarily having a substrate with plasmonic properties.[22,23]

SERS lending could open an avenue for new analytical applications for monitoring and identification. Future work needs to focus on a more in-depth experimental characterization of the mixed-metal substrate, as well as expanding the use of transition metals for detecting different analytes. The experimental challenge to overcome in future work is the determination of surface coverage, which would shed some light on the quantitive relationship between the borrowing and lending effects in mixed-metal SERS substrates.

■ ASSOCIATED CONTENT

Ⓢ Supporting Information

Experimental and computed Raman spectra of BPE, computed Raman spectra of $Ag_{14}M_4$·BPE, and of Ag_6M·Py, where M = {Ag, Pd, Pt}, and optimized geometries for all calculated systems. This material is available free of charge via the Internet at http://pubs.acs.org.

■ AUTHOR INFORMATION

Corresponding Author

*E-mail: aspuru@chemistry.harvard.edu.

Notes

The authors declare no competing financial interest.

■ ACKNOWLEDGMENTS

We acknowledge Prof. V. Narayanamurti, Drs. E. Diebold, J. Parkhill, S. Saikin, as well as D. Valencia for insightful discussions. We thank X. Zhou for help with simulations. This work was supported by the Defense Advanced Research Project Agency under Contract No. FA9550-08-1-0285 and by the Defense Threat Reduction Agency Contract No. HDTRA1-10-1-0046. This work was conducted while R.O.-A. was a Giorgio Ruffolo Fellow in the Sustainability Science Program at Harvard University. Support from CID and Italy's Ministry for Land, Environment, and Sea is gratefully acknowledged. The computations in this Article were carried out on the Odyssey cluster supported by the FAS Sciences Division Research Computing Group.

■ REFERENCES

(1) Fleischmann, M.; Hendra, P. J.; McQuillan, A. J. *Chem. Phys. Lett.* **1974**, *26*, 163−166.
(2) Jeanmaire, D. L.; Van Duyne, R. P. *J. Electroanal. Chem.* **1977**, *84*, 1−20.
(3) Albrecht, M. G.; Creighton, J. A. *J. Am. Chem. Soc.* **1977**, *99*, 5215−5217.
(4) Moskovits, M. *Rev. Mod. Phys.* **1985**, *57*, 783−826.
(5) Campion, A.; Kambhampati, P. *Chem. Soc. Rev.* **1998**, *27*, 241.
(6) Moskovits, M. *J. Raman Spectrosc.* **2005**, *36*, 485−496.
(7) *Surface-Enhanced Raman Scattering: Physics and Applications*; Kneipp, K., Moskovits, M., Kneipp, H., Eds.; Springer: Berlin, NY, 2006.
(8) Le Ru, E. C.; Etchegoin, P. G. *Principles of Surface-Enhanced Raman Spectroscopy and Related Plasmonic Effects*; Elsevier: Amsterdam; Boston, 2008.
(9) Camden, J. P.; Dieringer, J. A.; Zhao, J.; Van Duyne, R. P. *Acc. Chem. Res.* **2008**, *41*, 1653−1661.
(10) Stiles, P. L.; Dieringer, J. A.; Shah, N. C.; Van Duyne, R. P. *Annu. Rev. Anal. Chem.* **2008**, *1*, 601−626.
(11) Otto, A.; Mrozek, I.; Grabhorn, H.; Akemann, W. *J. Phys.: Condens. Matter* **1992**, *4*, 1143−1212.
(12) Otto, A. *J. Raman Spectrosc.* **2005**, *36*, 497−509.
(13) Jensen, L.; Zhao, L. L.; Schatz, G. C. *J. Phys. Chem. C* **2007**, *111*, 4756−4764.
(14) Jensen, L.; Aikens, C. M.; Schatz, G. C. *Chem. Soc. Rev.* **2008**, *37*, 1061−1073.
(15) Morton, S. M.; Jensen, L. *J. Am. Chem. Soc.* **2009**, *131*, 4090−4098.
(16) Saikin, S. K.; Olivares-Amaya, R.; Rappoport, D.; Stopa, M.; Aspuru-Guzik, A. *Phys. Chem. Chem. Phys.* **2009**, *11*, 9401−9411.
(17) Saikin, S. K.; Chu, Y.; Rappoport, D.; Crozier, K. B.; Aspuru-Guzik, A. *J. Phys. Chem. Lett.* **2010**, *1*, 2740−2746.
(18) Furtak, T. E.; Roy, D. *Phys. Rev. Lett.* **1983**, *50*, 1301−1304.
(19) Furtak, T. E.; Roy, D. *Surf. Sci.* **1985**, *158*, 126−146.
(20) Persson, B. N. J.; Zhao, K.; Zhang, Z. *Phys. Rev. Lett.* **2006**, *96*, 207401.
(21) Zayak, A. T.; Hu, Y. S.; Choo, H.; Bokor, J.; Cabrini, S.; Schuck, P. J.; Neaton, J. B. *Phys. Rev. Lett.* **2011**, *106*, 083003.
(22) Wang, X.; Shi, W.; She, G.; Mu, L. *J. Am. Chem. Soc.* **2011**, *133*, 16518−16523.
(23) Wang, X.; Shi, W.; She, G.; Mu, L. *Phys. Chem. Chem. Phys.* **2012**, *14*, 5891−5901.
(24) Tian, Z.-Q.; Ren, B.; Wu, D.-Y. *J. Phys. Chem. B* **2002**, *106*, 9463−9483.
(25) Leung, L. W. H.; Weaver, M. J. *J. Am. Chem. Soc.* **1987**, *109*, 5113−5119.
(26) Leung, L. W. H.; Weaver, M. J. *Langmuir* **1988**, *4*, 1076−1083.
(27) Zou, S.; Weaver, M. J.; Li, X. Q.; Ren, B.; Tian, Z. Q. *J. Phys. Chem. B* **1999**, *103*, 4218−4222.
(28) Weaver, M.; Zou, S.; Chan, H. *Anal. Chem.* **2000**, *72*, 38A−47A.
(29) Zou, S.; Weaver, M. J. *Anal. Chem.* **1998**, *70*, 2387−2395.
(30) Zou, S.; Williams, C. T.; Chen, E. K.-Y.; Weaver, M. J. *J. Am. Chem. Soc.* **1998**, *120*, 3811−3812.
(31) Mrozek, M. F.; Wasileski, S. A.; Weaver, M. J. *J. Am. Chem. Soc.* **2001**, *123*, 12817−12825.
(32) Wu, D.-Y.; Ren, B.; Xu, X.; Liu, G.-K.; Yang, Z.-L.; Tian, Z.-Q. *J. Chem. Phys.* **2003**, *119*, 1701−1709.
(33) Bao, L.; Mahurin, S. M.; Dai, S. *Anal. Chem.* **2004**, *76*, 4531−4536.
(34) Mahurin, S. M.; Bao, L.; Dai, S. *Isr. J. Chem.* **2006**, *46*, 329−336.
(35) Tian, Z.-Q.; Yang, Z.-L.; Ren, B.; Wu, D.-Y. SERS From Transition Metals and Excited by Ultraviolet Light. In *Surface-Enhanced Raman Scattering − Physics and Applications*; Kneipp, K., Moskovits, M., Kneipp, H., Eds.; Springer: Berlin, Heidelberg, 2006; Vol. *103*, pp 125−146.
(36) Tian, Z.-Q.; Yang, Z.-L.; Ren, B.; Li, J.-F.; Zhang, Y.; Lin, X.-F.; Hu, J.-W.; Wu, D.-Y. *Faraday Discuss.* **2006**, *132*, 159−170.
(37) Tian, Z.-Q.; Ren, B.; Li, J.-F.; Yang, Z.-L. *Chem. Commun.* **2007**, 3514−3534.
(38) Formo, E. V.; Zili, W.; Mahurin, S. M.; Dai, S. *J. Phys. Chem. C* **2011**, *115*, 9068−9073.

(39) Van Duyne, R. P.; Haushalter, J. P. *J. Phys. Chem.* **1983**, *87*, 2999−3003.
(40) Gersten, J.; Nitzan, A. *J. Chem. Phys.* **1980**, *73*, 3023−3037.
(41) Kennedy, B.; Spaeth, S.; Dickey, M. *J. Phys. Chem. B* **1999**, *103*, 3640−3646.
(42) Wasileski, S.; Zou, S.; Weaver, M. *Appl. Spectrosc.* **2000**, *54*, 761−772.
(43) Wolkow, R. A.; Moskovits, M. *J. Chem. Phys.* **1987**, *87*, 5858.
(44) *Quantum Chemistry Approaches to Chemisorption and Heterogeneous Catalysis*; Ruette, F., Ed.; Kluwer: Norwell, MA, 1992.
(45) Nørskov, J. K. *Rep. Prog. Phys.* **1990**, *53*, 1253−1295.
(46) Greeley, J.; Nørskov, J. K.; Mavrikakis, M. *Annu. Rev. Phys. Chem.* **2002**, *53*, 319−348.
(47) Somorjai, G. A.; Li, Y. *Introduction to Surface Chemistry and Catalysis*, 2nd ed.; Wiley: Hoboken, NJ, 2010.
(48) Schalnat, M. C.; Hawkridge, A. M.; Pemberton, J. E. *J. Phys. Chem. C* **2011**, *115*, 13717−13724.
(49) Zhao, L.; Jensen, L.; Schatz, G. C. *J. Am. Chem. Soc.* **2006**, *128*, 2911−2919.
(50) Diebold, E. D.; Mack, N. H.; Doorn, S. K.; Mazur, E. *Langmuir* **2009**, *25*, 1790−1794.
(51) Diebold, E. D.; Peng, P.; Mazur, E. *J. Am. Chem. Soc.* **2009**, *131*, 16356−16357.
(52) Perdew, J. P.; Ernzerhof, M.; Burke, K. *J. Chem. Phys.* **1996**, *105*, 9982−9985.
(53) Weigend, F.; Ahlrichs, R. *Phys. Chem. Chem. Phys.* **2005**, *7*, 3297−3305.
(54) Andrae, D.; Häußermann, U.; Dolg, M.; Stoll, H.; Preuß, H. *Theor. Chim. Acta* **1990**, *77*, 123−141.
(55) Adamo, C.; Cossi, M.; Scalmani, G.; Barone, V. *Chem. Phys. Lett.* **1999**, *307*, 265−271.
(56) Van Caillie, C.; Amos, R. D. *Chem. Phys. Lett.* **2000**, *328*, 446−452.
(57) Rappoport, D.; Furche, F. *J. Chem. Phys.* **2007**, *126*, 201104.
(58) Van Caillie, C.; Amos, R. D. *Phys. Chem. Chem. Phys.* **2000**, *2*, 2123−2129.
(59) Merrick, J. P.; Moran, D.; Radom, L. *J. Phys. Chem. A* **2007**, *111*, 11683−11700.
(60) Adamo, C.; Scuseria, G. E.; Barone, V. *J. Chem. Phys.* **1999**, *111*, 2889−2899.
(61) TURBOMOLE V5.10 2008, a development of University of Karlsruhe and Forschungszentrum Karlsruhe GmbH, 1989−2007, TURBOMOLE GmbH, since 2007; available from http://www.turbomole.com.
(62) Yang, W.; Hulteen, J.; Schatz, G.; Van Duyne, R. *J. Chem. Phys.* **1996**, *104*, 4313−4323.
(63) McMahon, J. J.; Babcock, G. *Spectrochim. Acta, Part A* **1982**, *38*, 1115−1122.
(64) Sun, G.; Grundmeier, G. *Thin Solid Films* **2006**, *515*, 1266−1274.
(65) Cai, W. B.; Ren, B.; Li, X. Q.; She, C. X.; Liu, F. M.; Cai, X. W.; Tian, Z. Q. *Surf. Sci.* **1998**, *406*, 9−22.
(66) McFarland, A. D.; Young, M. A.; Dieringer, J. A.; Van Duyne, R. P. *J. Phys. Chem. B* **2005**, *109*, 11279−11285.
(67) LeRu, E.; E., B.; Meyer, M.; Etchegoin, P. *J. Phys. Chem. C* **2007**, *111*, 13794−13803.
(68) Paoletti, P.; Vacca, A.; Arenare, D. *J. Phys. Chem.* **1966**, *70*, 193−196.
(69) Anderegg, G.; Wanner, H. *Inorg. Chim. Acta* **1986**, *113*, 101−108.
(70) Kukushkin, Y. N.; Yurinov, V. A. *Zh. Neorg. Khim.* **1973**, *18*, 182−188.
(71) Frontiera, R. R.; Henry, A.-I.; Gruenke, N. L.; Van Duyne, R. P. *J. Phys. Chem. Lett.* **2011**, *2*, 1199−1203.
(72) Hamelin, A.; Morin, S.; Richer, J.; Lipkowski, J. *J. Electroanal. Chem. Interfacial Electrochem.* **1989**, *272*, 241−252.
(73) Hamelin, A.; Morin, S.; Richer, J.; Lipkowski, J. *J. Electroanal. Chem. Interfacial Electrochem.* **1990**, *285*, 249−262.
(74) Zelenay, P.; Rice-Jackson, L. *Langmuir* **1990**, *6*, 974−979.
(75) Norrod, K.; Sudnik, L.; Rousell, D.; Rowlen, K. *Appl. Spectrosc.* **1997**, *51*, 994−1001.
(76) Liu, Y.; Fan, J.; Zhao, Y.-P.; Shanmukh, S.; Dluhy, R. A. *Appl. Phys. Lett.* **2006**, *89*, 173134.
(77) Driskell, J. D.; Shanmukh, S.; Liu, Y.; Chaney, S. B.; Tang, X.-J.; Zhao, Y.-P.; Dluhy, R. A. *J. Phys. Chem. C* **2008**, *112*, 895−901.
(78) Gui, Y.; Kuwana, T. *J. Electroanal. Chem. Interfacial Electrochem.* **1987**, *222*, 321−330.
(79) Dieringer, J. A.; McFarland, A. D.; Shah, N. C.; Stuart, D. A.; Whitney, A. V.; Yonzon, C. R.; Young, M. A.; Zhang, X.; Van Duyne, R. P. *Faraday Discuss.* **2006**, *132*, 9−26.